

1 Title (120 characters): Lmx1a drives Cux2 expression in the cortical hem through activation of a
2 conserved intronic enhancer.

3 Authors: Santiago P. Fregoso^{1,2}, Brett E. Dwyer², Santos J. Franco^{1,2*}

4 Author Affiliations: ¹Graduate Program in Cell Biology, Stem Cells and Development, University of
5 Colorado Graduate School - Anschutz Medical Campus, Aurora, CO 80045, USA.; ²Department of
6 Pediatrics, Section of Developmental Biology, University of Colorado School of Medicine - Anschutz
7 Medical Campus, Aurora, CO 80045, USA.

8

9 *Corresponding Author:

10 Santos Franco, PhD

11 University of Colorado School of Medicine - Anschutz Medical Campus

12 Department of Pediatrics

13 12800 East 19th Ave MS-8313

14 Aurora, CO 80045

15 E-mail: santos.franco@ucdenver.edu

16

17 Running Title: 32 characters: Lmx1a activates a Cux2 hem enhancer

18

19 Key words (3-6): Cux2, Lmx1a, cortical hem, corticogenesis, enhancer, patterning

20

21

22

23

24

25

26

27

28

29

30

31

32 **Summary Statement**

33 Analysis of a cortical hem-specific *Cux2* enhancer reveals role for *Lmx1a* as a critical upstream
34 regulator of *Cux2* expression patterns in neural progenitors during early forebrain development.

35

36

37

38

39

40

41

42

43

44

45

46

47

48

49

50

51

52

53

54

55

56 **Abstract**

57 During neocortical development, neurons are produced by a diverse pool of neural progenitors. A subset
58 of progenitors express the *Cux2* gene and are fate-restricted to produce certain neuronal subtypes, but
59 the upstream pathways that specify these progenitor fates remain unknown. To uncover the
60 transcriptional networks that regulate *Cux2* expression in the forebrain, we characterized a conserved
61 *Cux2* enhancer that we find recapitulates *Cux2* expression specifically in the cortical hem. Using a
62 bioinformatic approach, we found several potential transcription factor (TF) binding sites for cortical
63 hem-patterning TFs. We found that the homeobox transcription factor, *Lmx1a*, can activate the *Cux2*
64 enhancer *in vitro*. Furthermore, we show that multiple *Lmx1a* binding sites required for enhancer
65 activity in the cortical hem *in vivo*. Mis-expression of *Lmx1a* in neocortical progenitors caused an
66 increase in *Cux2*⁺-lineage cells. Finally, we compared several conserved human enhancers with cortical
67 hem-restricted activity and found that recurrent *Lmx1a* binding sites are a top shared feature.
68 Uncovering the network of TFs involved in regulating *Cux2* expression will increase our understanding
69 of the mechanisms pivotal in establishing *Cux2*-lineage fates in the developing forebrain.

70

71 **Introduction**

72 During forebrain development, neural progenitor cells give rise to many different types of neuronal and
73 glial cells that form the various telencephalic structures and circuits. This vast cellular diversity arises
74 through the interplay between early tissue patterning pathways and gene regulatory networks (GRNs).
75 Early in development, multiple tissue organizers and signaling centers provide morphogenic cues that
76 govern regional identity and size. Within these different regions, complex transcriptional programs
77 further diversify multipotent progenitor cells toward specific cell fates. The transcription factors (TFs)
78 that establish the different GRNs to specify cell fates often work by binding gene regulatory elements,
79 such as enhancers, to boost or suppress expression of target genes. Following transcriptional activation

80 of GRNs, neural progenitors divide and eventually differentiate into specified cells. A key to better
81 understanding forebrain development and function is to identify the signaling and transcriptional
82 networks that establish regional identity and subtype fate specification during embryonic development.

83 The TF Cut-like homeobox 2 (*Cux2*) is dynamically expressed in complex spatiotemporal
84 patterns in the developing mouse forebrain (Zimmer et al., 2004). During early brain development, a
85 subset of neural progenitors weakly express *Cux2* transcripts in a salt and pepper pattern (Franco et al.,
86 2012). We previously fate-mapped the lineage output of *Cux2*⁺ progenitors in the neocortex and found
87 that this subset of neural progenitors are fate-restricted to produce late-born corticocortical neurons in
88 upper layers (Franco et al., 2012; Gil-Sanz et al., 2015). Our studies indicated that *Cux2*⁺ progenitors in
89 the developing forebrain are committed to this fate even before the onset of neurogenesis. However, the
90 underlying mechanisms that restrict *Cux2*⁺ progenitors to specific cell fates remain largely unknown.
91 *Cux2* knockout mice do not display any significant phenotype with respect to progenitor cell fate
92 specification (Cubelos et al., 2008), implying that *Cux2*, while a useful marker for a fate-committed
93 progenitor population, does not necessarily instruct fate in this context. We reasoned that a deeper
94 understanding of *Cux2*⁺ cell fate commitment in forebrain progenitors could be achieved by uncovering
95 the upstream GRNs responsible for the complex patterns of *Cux2* expression. Interestingly, neural
96 progenitors in the dorsal telencephalic midline (DTM) strongly express *Cux2* in a more complete pattern
97 than progenitors in adjacent regions, suggesting that this forebrain region might contain critical
98 transcriptional regulators of the *Cux2* locus.

99 Previous studies have uncovered enhancers active in the developing mouse telencephalon,
100 including an 856 bp element in intron 2 of the *Cux2* genomic locus that could drive strong transgene
101 expression in the DTM (Hasenpusch-Theil et al., 2012; Visel et al., 2008). Here, we characterized this
102 element as an active enhancer in the developing forebrain and show that it is specifically active in the
103 cortical hem, but not in the adjacent hippocampus or neocortex. We further analyzed this enhancer for

104 possible upstream regulators of *Cux2* expression. Among several bioinformatically identified candidates,
105 we tested several transcription factors known to function in or be expressed within the cortical hem.
106 Using an *in vitro* approach, we demonstrate that *Lmx1a* is a strong activator of the *Cux2* hem-specific
107 enhancer. Additionally, *in vivo* *Lmx1a* gain-of-function in the neocortex, a region normally devoid of
108 *Lmx1a* expression, increased the proportion of *Cux2*⁺ cells. Finally, we analyzed other enhancers that
109 exhibit specific activity in the cortical hem and identify recurrent *Lmx1a* binding sites as a common
110 motif shared between these distinct hem-specific enhancers. Our results suggest *Lmx1a* functions as an
111 upstream regulator of a conserved *Cux2* enhancer in the cortical hem, and raise the possibility that
112 *Lmx1a* is a critical TF in the GRN that specifies cortical hem fate.

113

114 **Results**

115 **Early forebrain expression of *Cux2* begins at the dorsal telencephalic midline**

116 To better understand when and where the earliest transcriptional regulators of *Cux2* are active in the
117 developing telencephalon, we sought to define the temporal and spatial patterns of *Cux2* gene
118 expression. We crossed *Cux2*^{Cre/+} mice to the *Ai9* Cre-reporter line and used recombination (tdTomato⁺)
119 as a readout of the cumulative transcriptional history of the *Cux2* genomic locus. *Cux2*^{Cre/+}; *Ai9*^{fl/+} brains
120 were analyzed at E9.5, 10.5, 12.5 and 14.5 (Fig 1). We found that the earliest consistent pattern of
121 recombined cells in the forebrain first appeared in the dorsal telencephalic midline (DTM) at ~ E9.5
122 (Fig. 1A). At this age, a few recombined cells also began to appear scattered very sparsely throughout
123 the adjacent neocortical neuroepithelium (Fig. 1A). By E10.5, the entire DTM was recombined, and the
124 number of tdTomato⁺ neuroepithelial cells was increased in the neocortex (Fig. 1B). At E12.5 and
125 E14.5, the DTM is reorganized to comprise 2 distinct structures: the cortical hem and choroid plexus
126 epithelium (Grove et al., 1998). Essentially all cells in the cortical hem and choroid plexus were
127 recombined at E12.5 (Fig. 1C) and E14.5 (Fig. 1D). In contrast, only a fraction of cells in the adjacent

128 hippocampal primordium and neocortex were recombined (Fig. 1C-D). In fact, we observed a strikingly
129 sharp border of complete-to-sparse recombination at the boundary between the cortical hem and the
130 hippocampal primordium. These data indicate that forebrain activation of the *Cux2* locus occurs earliest
131 and most uniformly in the DTM, including the cortical hem and choroid plexus.

132

133 ***Cux2* regulatory element contains characteristics of an active enhancer and recapitulates the**
134 **endogenous *Cux2* expression pattern in the cortical hem**

135 Non-coding gene regulatory elements, such as enhancers, can act as critical platforms for TFs that drive
136 cell fate decisions (Pattabiraman et al., 2014). To gain insights into some of the transcriptional programs
137 that specify area and subtype fate in the telencephalon, we sought to identify enhancers that could
138 recapitulate *Cux2* expression in the developing forebrain. A previous study identified an 856 base pair
139 (bp) region within the human *Cux2* gene (hs611) that exhibits extreme human-rodent sequence
140 conservation, suggesting an important functional role for this non-coding element (Visel et al., 2008).
141 Indeed, both the human element (Visel et al., 2008) and the corresponding murine region (Hasenpusch-
142 Theil et al., 2012) can drive restricted expression of a *lacZ* reporter gene in transgenic mouse embryos,
143 indicating their role as functional enhancer elements. This enhancer lies within intron 2 of the *Cux2* gene
144 (Fig. 2A) and has characteristics of an active enhancer in E14.5 forebrain tissue, including a prominent
145 DNaseI hypersensitivity peak and histone marks H3K4me1 and H3K27ac, indicative of open,
146 transcriptionally active chromatin (Fig. 2B).

147 Interestingly, the human and murine elements both exhibited expression patterns in the
148 developing forebrain similar to that of *Cux2*, including strong expression in the DTM (Hasenpusch-Theil
149 et al., 2012; Visel et al., 2008). To better characterize the expression pattern of this candidate enhancer
150 in the developing forebrain, we first cloned the 856 bp murine region into an expression vector (Wilken
151 et al., 2015) with a minimal promoter (TATA box) driving Cre recombinase. We then introduced the

152 plasmid into the developing forebrain of *Ai9* Cre-reporter mice at E12.5, using *in utero* electroporation
153 (Fig. 3A). We co-electroporated a plasmid expressing GFP from the ubiquitously-expressed synthetic
154 CAG promoter (Niwa et al., 1991) as a marker of electroporated cells (Fig. 3A). Electroporations were
155 performed to target different regions of the telencephalon, including the cortical hem, hippocampal
156 primordium, and neocortex. We analyzed patterns of GFP expression and Cre-mediated recombination
157 (tdTomato expression) at E14.5. As controls, we compared recombination patterns in the
158 *Cux2*Enhancer-Cre electroporations to those of the minimal promoter construct alone (MINp-Cre, no
159 enhancer) or with a strong and ubiquitous promoter (CAG-Cre). We found that recombined tdTomato⁺
160 cells in the MINp-Cre electroporations were very sparse in the DTM (Fig. 3B), hippocampus and the
161 neocortex (Fig. 3E), consistent with weak expression from the TATA box alone. Conversely, the CAG-
162 Cre construct drove recombination ubiquitously throughout the electroporated regions, including in the
163 cortical hem, hippocampus and neocortex (Fig. 3C,F). Interestingly, recombination in the
164 *Cux2*Enhancer-Cre electroporations was almost completely restricted to the cortical hem (Fig. 3D). Very
165 few tdTomato⁺ cells were present in the hippocampus (Fig. 3D) or the neocortex (Fig. 3G). These data
166 demonstrate that the activity of this *Cux2* enhancer is restricted within the telencephalon to the cortical
167 hem, recapitulating a specific aspect of the complex endogenous *Cux2* expression pattern.

168

169 **Developmentally expressed cortical hem transcription factors, *Lmx1a* and *Emx2*, activate the**
170 ***Cux2* enhancer.**

171 As pioneering regulators of development, TFs often control gene expression by acting on enhancers. To
172 identify candidate transcriptional regulators of *Cux2* expression in the cortical hem, we analyzed the
173 hem-specific enhancer sequence for predicted TF binding sites using the JASPAR (Khan et al., 2018)
174 database with a ‘predicted’ and ‘consensus’ match threshold of 80% or higher. We identified ten
175 recurring 8 base-pair clusters that contained consensus binding sequences for a set of known cortical

176 hem-expressed TFs, including *Emx2*, *Lmx1a* and *Msx1* (Fig. 4A-B). *Lmx1a* and *Msx1* are expressed in
177 the DTM (Fig. 4B) at E8.5 and E9.5, respectively, and their expression continues into adulthood (Failli
178 et al., 2002; Furuta et al., 1997). *Emx2* is expressed by neural progenitors in the hippocampus and
179 neocortex beginning at E8.5, with the dorsomedial-most expression domain extending into the cortical
180 hem (Fig. 4B) (Simeone et al., 1992a; Simeone et al., 1992b; Yoshida et al., 1997). As key players in
181 telencephalic patterning, these TFs serve as ideal candidates for regulating *Cux2* expression in the
182 cortical hem during early forebrain development. To test whether any of these TFs can activate the hem-
183 specific *Cux2* enhancer, the enhancer element was cloned into the minimal promoter vector driving
184 nuclear mCherry expression (Fig 5A). cDNAs for the candidate TFs were cloned into the bicistronic
185 expression vector pCIG (Hand et al., 2005), which drives expression of both the TF and GFP from the
186 CAG promoter. Each candidate TF plasmid was co-transfected with the *Cux2*-Enhancer-mCherry
187 plasmid into murine immortalized neuroectodermal (NE-4C) cells (Schlett and Madarász, 1997). 24
188 hours after transfection, mRNA was collected from the cells and analyzed by RT-qPCR for levels of the
189 *mCherry* reporter transcript (Fig. 5A). Compared to the pCIG empty vector negative control, *Emx2* and
190 *Lmx1a* significantly upregulated expression from the *Cux2* enhancer (Fig. 5B). In contrast, *Msx1* did not
191 change *Cux2* enhancer-driven *mCherry* levels compared to control (Fig. 5B).

192

193 **Activation of the *Cux2* enhancer in the cortical hem requires *Lmx1a* binding sites.**

194 Our *in silico* data predicted multiple binding sites for *Emx2* and *Lmx1a* that overlapped each other (Fig.
195 4B), which correlated well with our *in vitro* studies demonstrating that these factors can activate the
196 *Cux2* enhancer (Fig. 5B). To directly test whether these putative TF binding sequences were required for
197 enhancer activation, we generated a mutant enhancer construct in which the central 8 base pairs of the
198 predicted binding sites were mutated (Fig. 5C) and the mutant *Cux2*Enhancer-mCherry plasmid was
199 tested for activation by *Emx2* and *Lmx1a*. In contrast to the wild-type *Cux2* enhancer, the mutated

200 version was no longer activated by Lmx1a (Fig. 5C). Surprisingly, Emx2 was still able to upregulate
201 expression from the mutated enhancer (Fig. 5C), raising the possibility of other more critical Emx2
202 binding sites within the enhancer.

203 We next tested the activity of the mutated enhancer *in vivo* by *in utero* electroporation of the
204 mutated enhancer driving Cre recombinase into *Ai9* reporter embryos (Fig. 6A). As we observed
205 previously, the wild-type *Cux2*-Enhancer-Cre drove recombination specifically and robustly in the
206 cortical hem (Fig. 6B). In contrast, the TF binding site mutant *Cux2*-Enhancer-Cre construct was unable
207 to drive any recombination at all in the cortical hem (Fig. 6C). Together with our *in vitro* studies, these
208 *in vivo* data indicate that the binding sites for Lmx1a are required for activity of the *Cux2* enhancer and
209 that Lmx1a is an important transcriptional regulator of the *Cux2* enhancer in the cortical hem. The fact
210 that mutating the enhancer abolished expression *in vivo*, but not activation by Emx2 *in vitro*, indicates
211 that Emx2 may not be a critical regulator of the *Cux2* hem enhancer *in vivo*.

212

213 **Lmx1a gain of function increases endogenous *Cux2* expression in the neocortex.**

214 In the developing telencephalon, Lmx1a is expressed strongly throughout the DTM, where it functions
215 to promote cortical hem fate and suppress hippocampal and neocortical fate (Caronia-Brown et al.,
216 2014; Chizhikov et al., 2010; Failli et al., 2002). The sharp border of *Lmx1a* expression between the
217 cortical hem and hippocampus is very similar to that of *Cux2* (Fig. 7A), which is expressed strongly
218 throughout the cortical hem but only weakly in a limited number of progenitors and neurons in the
219 hippocampus and neocortex (Fig. 1). Since Lmx1a is not expressed at all in the developing neocortex
220 where *Cux2* expression is initially weak, this provided us an opportunity to assess whether mis-
221 expression of Lmx1a in the neocortex is sufficient to upregulate endogenous *Cux2* expression. To test
222 this possibility, we electroporated our CAG-Lmx1a-IRES-GFP construct into the neocortex of *Cux2*^{Cre/+};
223 *Ai9*^{fl/+} embryos *in utero* at E12.5 (Fig. 7B). We allowed the embryos to continue developing until E14.5

224 and analyzed the percentage of electroporated cells (GFP⁺) that belonged to the *Cux2* lineage
225 (tdTomato⁺). Compared to the CAG-IRES-GFP control (Fig. 7C-D), *Lmx1a* mis-expression resulted in a
226 statistically significant ($p = 0.0001$) 2-fold increase in tdTomato⁺ cells within the electroporated
227 population (Fig. 7E-G). These data support a role for *Lmx1a* in promoting endogenous *Cux2* expression
228 in the early developing telencephalon.

229

230 **Multiple *Lmx1a* binding sites are a shared feature among cis-regulatory elements active in the** 231 **cortical hem**

232 Previous work has revealed a number of forebrain enhancers, including some that appear to have
233 restricted cortical hem activity similar to the murine *Cux2* enhancer (Pattabiraman et al., 2014; Visel et
234 al., 2008). Human enhancer elements hs411, hs611 and hs643 can drive cortical hem-specific lacZ
235 expression in transgenic mouse embryos (Fig 8A-C). We reasoned that all three enhancers might share
236 features that regulate their activity through a common mechanism, given their very similar spatial and
237 temporal transcriptional activity. To uncover common features between hs611, hs411 and hs643, the
238 sequences of all three genomic regions together with the murine *Cux2* hem enhancer were analyzed
239 using Analysis of Motif Enrichment (McLeay and Bailey, 2010) through the MEME Suite web portal
240 (<http://meme-suite.org/tools/ame>). Compared to 1004 shuffled control sequences, the most enriched
241 motif shared by all four elements was a TTAATTAA motif ($p = 1.48e-6$ by Fisher's exact test) that was
242 identified as an *Lmx1a* consensus binding motif by JASPAR, Jolma and Uniprobe databases (Fig. 8D).
243 We next used the JASPAR database (>85% threshold) to search all three human enhancer elements for
244 putative *Lmx1a* binding sites. Similar to the murine *Cux2* cortical hem enhancer, hs611, hs411 and
245 hs642 are all predicated to contain multiple high-threshold *Lmx1a* binding sites (Fig. 8E). As a common
246 feature among cortical hem enhancers, the presence of multiple *Lmx1a* binding sites may indicate that
247 *Lmx1a* sits near the top of the GRN active in the developing cortical hem, perhaps as a pioneering TF.

248

249 **Discussion**

250 Using a combination of *in silico*, *in vitro* and *in vivo* approaches, we characterized a *Cux2* gene
251 regulatory element with the goal of uncovering key TFs involved in the transcriptional regulation of
252 *Cux2* in neural progenitors. We showed that this *Cux2* enhancer recapitulates a specific aspect of the
253 complex *Cux2* expression pattern in the developing forebrain, namely strong and precise expression in
254 the cortical hem. Our further analysis uncovered the LIM homeobox transcription factor, *Lmx1a*, as a
255 positive regulator of the *Cux2* cortical hem enhancer. Comparison of 3 cortical hem-specific human
256 enhancer elements revealed that recurring *Lmx1a* binding sites is the top shared motif, raising the
257 possibility that *Lmx1a* is master transcriptional regulator of the GRN that controls cortical hem identity.

258

259 ***Cux2* expression as a tool to uncover regulators of cell-fate decisions**

260 We previously identified a subset of neural progenitors in the developing forebrain that are fate-
261 restricted to produce only corticocortical projection neurons in the neocortex (Franco and Müller, 2013;
262 Franco et al., 2012; Gil-Sanz et al., 2015). These progenitors can be identified by expression of the
263 transcription factor, *Cux2*, and lineage-traced using *Cux2-Cre* and *Cux2-CreERT2* knock-in mice.
264 Although *Cux2* itself does not appear to control cell fate decisions in the forebrain (Cubelos et al., 2008;
265 Cubelos et al., 2010), its restricted expression in defined subsets of neural progenitors may be a useful
266 tool for uncovering transcriptional regulators of cell fate during forebrain patterning. The *Cux2*
267 expression pattern in the developing forebrain is complex and dynamic (Franco et al., 2012; Gil-Sanz et
268 al., 2015; Zimmer et al., 2004), suggesting that control of the *Cux2* locus may involve multiple
269 transcriptional regulatory mechanisms. Using our *Cux2-Cre* mice crossed to a Cre-reporter line, we
270 identified the DTM as one of the earliest sites of *Cux2* expression in the developing forebrain. In
271 contrast to the salt-and-pepper pattern of *Cux2* expression in the adjacent hippocampus and neocortex,

272 we find that essentially all neural progenitors in the cortical hem belong to the *Cux2* lineage. This raised
273 the interesting possibility that *Cux2* expression in different parts of the developing forebrain are
274 controlled by distinct mechanisms. Identification of the various cis-regulatory elements that drive
275 differential *Cux2* expression, and the transcription factors that regulate these elements, may therefore
276 lead to a better understanding of the GRNs that control tissue patterning and subtype fate specification in
277 the developing forebrain.

278

279 **Identification and characterization of a cortical hem-specific *Cux2* enhancer**

280 Previous studies identified genomic regions within intron 2 of the human and murine *Cux2* genes that
281 can recapitulate *Cux2* expression in the DTM of transgenic mice (Hasenpusch-Theil et al., 2012; Visel et
282 al., 2008). We found that the murine *Cux2* element exhibits features of an active enhancer in the E14.5
283 forebrain, including DNaseI hypersensitivity and histone modifications associated with transcriptionally
284 active chromatin. This region also displays high levels of conservation from humans to chickens,
285 pointing toward an important functional role. Using *in utero* electroporation to test the *in vivo* activity of
286 this region, we show that it drives expression specifically and robustly in the cortical hem
287 neuroepithelium, but not in progenitors in the adjacent hippocampus or neocortex. These data indicate
288 that this element is a developmentally active enhancer specific for the cortical hem. It will be interesting
289 in future studies to determine which features of this enhancer are required for *Cux2* expression in the
290 cortical hem, and whether this regulatory element is active in other *Cux2* expression domains that share
291 features with the cortical hem, such as the rhombic lip in the hindbrain (Capaldo and Iulianella, 2016).

292

293 **Lmx1a is a critical regulator of the *Cux2* hem-specific enhancer**

294 Using a bioinformatics approach, we identified several putative TF binding sites in the *Cux2* enhancer.
295 As known regulators of cortical hem development (Chizhikov et al., 2010; Tole et al., 2000), *Emx2*,

296 Lmx1a and Msx1 comprised a promising group of candidate TFs with the potential to regulate the *Cux2*
297 enhancer in the cortical hem. We did not identify any effect of Msx1 on activity of the *Cux2* enhancer *in*
298 *vitro*, indicating it may not be a direct regulator of *Cux2* cortical hem expression. On the other hand,
299 both Emx2 and Lmx1a activated transcription from the *Cux2* enhancer. The majority of the predicted
300 Emx2 and Lmx1a binding sites overlapped each other, reflective of the similarity of their consensus
301 binding motifs. Interestingly, mutation of several of these putative binding sites drastically reduced
302 responsiveness of the enhancer to Lmx1a, but not to Emx2. This may suggest substantial redundancy in
303 the Emx2 binding sites in the *Cux2* enhancer, or that the remaining Emx2 binding sites are more critical.
304 Importantly, the mutated enhancer showed no activity in the cortical hem, suggesting that binding of
305 Lmx1a, but not Emx2, is critical for enhancer activation *in vivo*. This would be in line with our further
306 experiments showing that the *Cux2* enhancer is not active in the neocortex, where Emx2 is strongly
307 expressed but Lmx1a is absent.

308 In further support of Lmx1a as an activator of *Cux2* expression, we found that mis-expressing
309 Lmx1a in the neocortex results in an increase in *Cux2*⁺ cells. Although this assay does not allow us to
310 determine whether the increase results from direct activation of the cortical hem enhancer, our data point
311 to Lmx1a as being sufficient to activate *Cux2* expression in the developing forebrain. Interestingly,
312 Lmx1a mis-expression in the neocortex did not drive recombination in all cells in the electroporated
313 region, in contrast to the complete recombination pattern seen in the cortical hem of *Cux2-Cre* mice.
314 This result could simply be due to insufficient levels or duration of Lmx1a expression, or it may suggest
315 the presence of additional factors that regulate *Cux2* expression. For example, Lmx1a may require a
316 transcriptional co-activator for maximum activity that is missing from the neocortex, or perhaps there is
317 an unidentified transcriptional repressor of the *Cux2* enhancer that is expressed specifically in the
318 neocortex. Further studies will be required to fully elucidate the mechanisms that control the complex
319 expression pattern of *Cux2* in the developing forebrain.

320

321 **Lmx1a as a common activator of cortical hem GRNs**

322 When we compared the murine and human *Cux2* enhancers to two other conserved human elements that
323 drive expression in the cortical hem, we found that the top motif enriched in all four enhancers
324 corresponds to the *Lmx1a* consensus binding site. Together with the fact that *Lmx1a* is one of the
325 earliest markers of the DTM (Failli et al., 2002; Mangale et al., 2008), these data suggest that *Lmx1a*
326 may sit near the top of the GRN involved in regulating cortical hem cell fate. In line with this idea,
327 cortical hem identity is lost in *dreher* mutant mice in which *Lmx1a* is inactivated by a missense mutation
328 (Chizhikov et al., 2010). The sharp border of *Lmx1a* expression between the cortical hem and adjacent
329 hippocampal primordium further make it an ideal candidate for establishing precise patterns of gene
330 expression during early patterning of the developing forebrain. An important unanswered question is
331 what lies upstream of *Lmx1a* during these early patterning stages. Previous work has reported that
332 *Lmx1a* expression can be activated by BMP4 in the developing forebrain (Srinivasan et al., 2014;
333 Watanabe et al., 2016). As a morphogenetic pathway that is specifically expressed within the cortical
334 hem and choroid plexus, BMP signaling could potentially initiate the *Lmx1a*-dependent GRN that leads
335 to specific DTM fates. Interestingly, previous studies have reported that upregulation of BMP signaling
336 both in the developing chick olfactory epithelium (Wittmann et al., 2014) and murine mandibular neural
337 crest cells (Bonilla-Claudio et al., 2012) results in significant upregulation of *Cux2* expression.
338 Additionally, *Cux2* expression appears coincident with BMP4 within the mesenchyme of the developing
339 mouse limb bud (Iulianella et al., 2003). How BMPs activate *Cux2* expression in these contexts has not
340 been determined, but it would be interesting to test whether BMP signaling can drive *Cux2* expression in
341 multiple tissues through *Lmx1a*-mediated activation of the conserved enhancer.

342

343 **Conclusions**

344 In this study we identify a conserved enhancer and its transcriptional activator, *Lmx1a*, as an
345 important mechanism for driving restricted expression of *Cux2* in the developing forebrain. We further
346 show that recurrent *Lmx1a* binding sites are a common motif shared in multiple enhancers with
347 similarly restricted activities. These studies provide a template for future studies aimed at identifying
348 other *Cux2* cis-regulatory elements that control its complex expression during forebrain development,
349 and the ultimately the upstream GRNs that specify different cell fates among the forebrain progenitor
350 pool.

351

352 **Materials and Methods**

353 *Animals.* Mice used for experiments were housed and handled in accordance with protocols approved by
354 the UC Anschutz Medical Campus IACUC committee. The following mouse lines were used in this
355 study: *Cux2-Cre* (Franco et al., 2012; 2011(Franco et al., 2012; Franco et al., 2011; Gil-Sanz et al.,
356 2015)), *Ai9* (Madisen et al., 2010) and C57BL/6J. Embryos were produced from timed-pregnant
357 females, with noon on the day of plug being designated E0.5.

358 *Plasmids and In Utero Electroporation.* The murine *Cux2* enhancer was cloned from the endogenous
359 genomic locus (NCBI37/mm9 chr5:122,482,512-122,483,367) using a Gblock (IDT) with 5' and 3'
360 arms homologous to the multiple cloning site in the backbone vector. The Gblock was cloned by Gibson
361 assembly into the pMinp vector (Wilken et al., 2015), immediately upstream of the TATA box. mCherry
362 or Cre recombinase with a nuclear localization signal (Lewandoski and Martin, 1997) were cloned
363 immediately downstream of the TATA box. To generate the TF binding site mutant version of the *Cux2*
364 enhancer, we synthesized a Gblock in which the central 8 base pairs of each putative binding site was
365 mutated to 5' AAGCGCAA3'. Transcription factor cDNAs were either obtained from Addgene (*Lmx1a*:
366 45070, *Msx1*: 34998) or from IDT as Gene blocks (*Emx2*) and cloned into the *SacI* and *XmaI* sites of

367 the pCIG vector (Hand et al., 2005), between the CAG promoter and the IRES-GFP cassette. In utero
368 electroporation of plasmids (0.5-1mg/ml) were carried out as previously described (Franco et al., 2012;
369 Gil-Sanz et al., 2013) on E12.5 embryos of timed-pregnant mice. Embryos were harvested for analysis
370 at E14.5.

371 *Immunohistochemistry.* Brains from E9.5-14.5 embryos were dissected and fixed for 2 hours at room
372 temperature in 4% paraformaldehyde. Forebrains were sectioned on a vibrating microtome (Leica
373 VT1200S) at 100 μ m increments, or on a cryostat (Leica CM1520) at 15-30 μ m increments.
374 Immunohistochemistry was performed on tissue sections as described previously (Winkler et al., 2018)
375 using the following antibodies: rabbit anti-Lmx1a (1:1000, Millipore, RRID:AB_10805970), rabbit anti-
376 RFP (1:500, LifeSpan Biosciences, RRID:AB_945213). Donkey secondary antibodies conjugated to
377 Alexa Fluor 488, Rhodamine Red-X, or Alexa Fluor 647 were purchased from Jackson
378 ImmunoResearch and used at 1:500. Sections were imaged using a Zeiss LSM 780 confocal microscope.

379 *Cell culture and qRT-PCR:* Experiments were performed using the immortalized mouse
380 neuroectodermal NE-4C cells (ATCC CRL-2925), grown in Dulbecco's minimal essential media
381 (MEM; Corning 10-010-CV) with 4mM L-glutamine (Invitrogen), 10% fetal bovine serum (FBS)
382 (Invitrogen) and Penicillin (0.0637g/L)-Streptomycin (0.1g/L). Cells were plated on 12 well plates and
383 grown to ~70% confluency prior to transfection. Cells were transfected with either CAG-Emx2, Lmx1a
384 or Msx1-IRES-GFP, together with *Cux2*Enhancer-mCherry or TF binding site mutated *Cux2*Enhancer-
385 mCherry for 4-6 hrs with Lipofectamine 3000 (Invitrogen), with subsequent media change. 24 hrs
386 following transfection, RNA was isolated from cells with an RNeasy Plus Kit (Qiagen) and reverse
387 transcribed into cDNA using an iScript RT Kit (Bio-Rad). Expression of *mCherry*, *GFP*, and
388 housekeeping gene *Cyclophilin A* was assessed by qRT-PCR (Bio-Rad CFX Connect R-T System). Fold
389 change was calculated by the delta-CT method for both *GFP* and *mCherry*, relative to *Cyclophilin A*.

390 Fold changes of *mCherry* mRNA were normalized to those of *GFP*, to account for variations in
391 transfection efficiency. The following primers were used: *Cyclophilin A* forward:
392 GAGCTGTTTGCAGACAAAGTTC, *Cyclophilin A* reverse: CCCTGGCACATGAATCCTGG, *eGFP*
393 forward: ACGTAAACGGCCACAAGTTC, *eGFP* reverse: AAGTCGTGCTGCTTCATGTG, *mCherry*
394 forward: GATAACATGGCCATCATCAAGGA, *mCherry* reverse: CGTGGCCGTTACGGAG.

395 *Quantitative analysis of Lmx1a gain of function.* CAG-Lmx1a was electroporated into cortices of E12.5
396 *Cux2^{Cre/+};Ai9^{fl/+}* embryos (n=3) followed by quantification of *Cux2* expression at E14.5. At least 3
397 histological sections from distinct rostro-caudal regions collected from 3 different animals were
398 analyzed in regions comprising primarily the somatosensory cortex. Single-plane confocal images were
399 used for quantification. *Cux2*⁺ cells were counted based on tdTomato expression from the recombined
400 *Ai9* allele while *Lmx1a* expressing cells were labeled by GFP expression. *Cux2*-expressing cells were
401 quantified as a percentage of those expressing *Lmx1a*. All analysis was performed using Fiji/ImageJ on
402 3-5 20x images per brain.

403 *Statistics.* As all comparisons made were between two groups, a two-tailed, two-sample equal or
404 unequal variance Student *t*-tests were used to analyze all data. Equality of variance was determined
405 using a Bartlett's Test. The standard error of the mean (SEM) is reported on all graphs.

406

407 Acknowledgments: We thank Joseph Brzezinski (University of Colorado – Anschutz Medical Campus)
408 for providing the minimal promoter plasmids.

409

410 Competing interests: The authors declare no competing financial interests.

411

412 Funding: This work was supported by the Children's Hospital Colorado Program in Pediatric Stem Cell
413 Biology and The Boettcher Foundation (S.J.F.).

414

415 **Figure Legends**

416

417 **Fig. 1. Spatiotemporal development of *Cux2* expression in murine telencephalic progenitors.**

418 Coronal sections of forebrains from *Cux2-Cre;Ai9* embryos showing recombination as a cumulative
419 readout of *Cux2* expression. Recombined cells express tdTomato (red). Sections were counterstained for
420 nuclei with DAPI (blue). Boxed insets show zoomed images of the dorsal midline (middle panels) or
421 neocortex (right panels). (A) E9.5: recombination is apparent in the dorsal-most region of the
422 telencephalic neural tube and in scattered cells in the telencephalon. (B) E10.5: recombination becomes
423 robust in the nascent cortical hem and choroid plexus, with salt-and-pepper recombination in the
424 neocortex. (C) E12.5: recombination is nearly ubiquitous in the cortical hem, while still mosaic in the
425 neocortex. (D) E14.5: recombination is complete in the cortical hem and much of the choroid plexus,
426 while the neocortex exhibits a still expanding, mosaic pattern. Scale bars: left panels, 200 μ m; middle
427 and right panels, 50 μ m, CH: cortical hem, CP: choroid plexus.

428

429 **Fig. 2. Genomic location and chromatin characteristics of a *Cux2* enhancer.** (A) Schematic of

430 murine *Cux2* genomic locus, showing the location of an 856 bp cis-regulatory element in the proximal
431 region of intron 2. (B) UCSC Genome Browser data demonstrating key enhancer characteristics for the
432 *Cux2* 856 bp element, including epigenetic marks H3K4me1 and H3K27ac, a prominent DNaseI
433 hypersensitivity peak, and a high degree of evolutionary conservation across taxa.

434

435 **Fig. 3. *Cux2* enhancer exhibits activity restricted to the cortical hem.** (A) Schematic of experimental

436 workflow: E12.5 *Ai9* reporter forebrains were electroporated *in utero* with constructs expressing Cre
437 recombinase driven by either a minimal TATA-box promoter (Minp), ubiquitous CAG promoter, or the
438 *Cux2* enhancer. CAG-GFP was co-electroporated to mark electroporated cells. Forebrains were
439 harvested at E14.5 for analysis. (B-D) Coronal sections of electroporated brains showing the dorsal

440 midline region. All electroporated cells express GFP (green) and recombined cells express tdTomato
441 (red). Boundary between the cortical hem and hippocampal primordium is marked by expression of
442 LMX1A protein (yellow). Sections were counterstained for nuclei with DAPI (blue). Electroporation of
443 Minp-Cre causes minimal recombination in the cortical hem and hippocampal primordium (B), whereas
444 CAG-Cre leads to ubiquitous recombination throughout the electroporated regions (C). *Cux2*Enhancer-
445 Cre drives robust recombination in the cortical hem, but not in the adjacent hippocampal primordium.
446 (E-G) Coronal sections of electroporated brains showing the neocortex. Similar to the dorsal midline,
447 Minp-Cre drives minimal recombination (E) and CAG-Cre drives ubiquitous recombination (F) in the
448 neocortex. The *Cux2* enhancer (G) exhibits no activity in the neocortex. Scale bars: B-D, 100 μ m; E-G,
449 50 μ m. CH, cortical hem; CP, choroid plexus; HP, hippocampal primordium.

450

451 **Fig. 4. The *Cux2* enhancer contains multiple predicted binding sites for forebrain-patterning**
452 **transcription factors expressed in the cortical hem.** (A) Schematic of the *Cux2* enhancer with
453 putative binding sites for Emx2, Lmx1a and Msx1, predicted from the JASPAR database at >80%
454 threshold. (B) JASPAR motifs for consensus binding site sequences of the candidate TFs. (C) Sagittal
455 sections from the Allen Brain Atlas *in situ* hybridization database showing mRNA expression of
456 candidate TFs in the cortical hem of E11.5 mouse forebrains. Scale bar, 400 μ m. Ctx, neocortex; CH,
457 cortical hem.

458

459 **Fig. 5. Lmx1a strongly activates the *Cux2* enhancer *in vitro*.** (A) Schematic of experimental
460 workflow. The *Cux2*Enhancer-mCherry plasmid was transfected into NE-4C cells together with either
461 empty pCIG vector (CAG-IRES-GFP) or pCIG that expresses candidate TFs (CAG-TF-IRES-GFP). The
462 effects of candidate TFs on expression of *Cux2*Enhancer-mCherry in NE-4C cells was quantified by
463 qPCR of *mCherry* mRNA. (B-C) qPCR quantification of *mCherry* transcripts. Bar graphs are fold

464 change (\pm SEM) over pCIG vector alone (dotted line), using the $\Delta\Delta$ Ct method. (B) Expression from the
465 *Cux2* enhancer is activated by expression of *Emx2* and *Lmx1a*, but not *Msx1*. (C) When putative TF
466 binding sites were mutated in the *Cux2* enhancer, *Emx2* could still activate transcription but the effects
467 of *Lmx1a* on transcription were greatly diminished.

468

469 **Fig. 6. TFBS-mutated *Cux2* enhancer activity abolished *in vivo*.** (A) Schematic of experimental
470 workflow. *Ai9* reporter embryos were electroporated *in utero* at E12.5 with either the wild-type
471 *Cux2*enhancer-Cre plasmid or the mutated version that is no longer activated by *Lmx1a*. CAG-GFP was
472 co-electroporated as a marker of the electroporated cells. Forebrains were harvested at E14.5 for analysis
473 of recombination. (B-C) Coronal sections of electroporated brains showing the dorsal midline region.
474 All electroporated cells express GFP (green) and recombined cells express tdTomato (red). Boundary
475 between the cortical hem and hippocampal primordium is marked by expression of LMX1A protein
476 (yellow). Sections were counterstained for nuclei with DAPI (blue). The wild-type *Cux2* enhancer
477 driving Cre led to robust recombination specifically in the cortical hem (B), whereas the TFBS-mutated
478 enhancer lost all activity in the cortical hem (C). Scale bars, 100 μ m. Abbreviations as in Fig. 3.

479

480 **Fig. 7. *Lmx1a* gain-of-function in the neocortex increases the number of *Cux2*⁺ cells.** (A) Schematic
481 of experimental workflow. *Cux2-Cre;Ai9* embryos were electroporated at E12.5 with a constitutive
482 *Lmx1a* expression plasmid. Forebrains were harvested at E14.5 for quantification of the percentage of
483 electroporated cells that were recombined. (B) Coronal section of a neocortex electroporated with
484 empty vector control (pCIG). Electroporated cells are GFP⁺ (green), and recombined cells from the
485 *Cux2*-Cre lineage are tdTomato⁺ (red). Sections were counterstained for nuclei with DAPI (blue). (C)
486 Magnified inset from (B) showing electroporated *Cux2*-lineage cells. (D) Coronal section of a neocortex
487 electroporated with the *Lmx1a* expression vector. GFP⁺ cells are mis-expressing *Lmx1a*. (E) Magnified

488 inset from (D) showing that Lmx1a gain-of-function results in an increased percentage of electroporated
489 cells that are recombined. (F) Quantification showing percent (\pm SEM) of electroporated cells (GFP⁺)
490 that are recombined (tdTomato⁺) in control vs Lmx1a electroporations. Scale bars: B and D, 100 μ m; C
491 and E, 25 μ m.

492

493 **Fig. 8. Lmx1a binding sites are a common feature of enhancers active in the developing cortical**

494 **hem.** (A-C) Examples of human enhancer elements driving LacZ expression in transgenic mouse

495 embryos. Whole mount staining images from the Vista Enhancer Browser show activity of hs411 (A),

496 hs611 (B) and hs643 (C) in the cortical hem region. (D) Analysis of Motif Enrichment identified Lmx1a

497 consensus binding sites as the most significantly enriched motif in the 4 hem-expressed enhancers. (E)

498 Using the JASPAR database, all four cortical hem enhancers were predicted to contain 7 or more high-

499 threshold Lmx1a binding sites.

500

501 **References**

- 502 **Bonilla-Claudio, M., Wang, J., Bai, Y., Klysik, E., Selever, J. and Martin, J. F.** (2012). Bmp
503 signaling regulates a dose-dependent transcriptional program to control facial skeletal development.
504 *Development* **139**, 709–719.
- 505 **Capaldo, E. and Iulianella, A.** (2016). Cux2 serves as a novel lineage marker of granule cell layer
506 neurons from the rhombic lip in mouse and chick embryos. *Dev Dyn* **245**, 881–896.
- 507 **Caronia-Brown, G., Yoshida, M., Gulden, F., Assimacopoulos, S. and Grove, E. A.** (2014). The
508 cortical hem regulates the size and patterning of neocortex. *Development* **141**, 2855–2865.
- 509 **Chizhikov, V. V., Lindgren, A. G., Mishima, Y., Roberts, R. W., Aldinger, K. A., Miesegaes, G. R.,**
510 **Curle, D. S., Monuki, E. S. and Millen, K. J.** (2010). Lmx1a regulates fates and location of cells
511 originating from the cerebellar rhombic lip and telencephalic cortical hem. *Proc Natl Acad Sci USA*
512 **107**, 10725–10730.
- 513 **Cubelos, B., Sebastián-Serrano, A., Beccari, L., Calcagnotto, M. E., Cisneros, E., Kim, S., Dopazo,**
514 **A., Alvarez-Dolado, M., Redondo, J. M., Bovolenta, P., et al.** (2010). Cux1 and Cux2 regulate
515 dendritic branching, spine morphology, and synapses of the upper layer neurons of the cortex.
516 *Neuron* **66**, 523–535.
- 517 **Cubelos, B., Sebastián-Serrano, A., Kim, S., Moreno-Ortiz, C., Redondo, J. M., Walsh, C. A. and**
518 **Nieto, M.** (2008). Cux-2 controls the proliferation of neuronal intermediate precursors of the
519 cortical subventricular zone. *Cereb Cortex* **18**, 1758–1770.
- 520 **Failli, V., Bachy, I. and Rétaux, S.** (2002). Expression of the LIM-homeodomain gene Lmx1a (dreher)
521 during development of the mouse nervous system. *Mech Dev* **118**, 225–228.
- 522 **Franco, S. J. and Müller, U.** (2013). Shaping our minds: stem and progenitor cell diversity in the
523 mammalian neocortex. *Neuron* **77**, 19–34.
- 524 **Franco, S. J., Gil-Sanz, C., Martinez-Garay, I., Espinosa, A., Harkins-Perry, S. R., Ramos, C. and**
525 **Müller, U.** (2012). Fate-restricted neural progenitors in the mammalian cerebral cortex. *Science*
526 **337**, 746–749.
- 527 **Franco, S. J., Martinez-Garay, I., Gil-Sanz, C., Harkins-Perry, S. R. and Müller, U.** (2011). Reelin
528 regulates cadherin function via Dab1/Rap1 to control neuronal migration and lamination in the
529 neocortex. *Neuron* **69**, 482–497.
- 530 **Furuta, Y., Piston, D. W. and Hogan, B. L.** (1997). Bone morphogenetic proteins (BMPs) as
531 regulators of dorsal forebrain development. *Development* **124**, 2203–2212.
- 532 **Gil-Sanz, C., Espinosa, A., Fregoso, S. P., Bluske, K. K., Cunningham, C. L., Martinez-Garay, I.,**
533 **Zeng, H., Franco, S. J. and Müller, U.** (2015). Lineage Tracing Using Cux2-Cre and Cux2-
534 CreERT2 Mice. *Neuron* **86**, 1091–1099.
- 535 **Gil-Sanz, C., Franco, S. J., Martinez-Garay, I., Espinosa, A., Harkins-Perry, S. and Müller, U.**
536 (2013). Cajal-Retzius cells instruct neuronal migration by coincidence signaling between secreted

- 537 and contact-dependent guidance cues. *Neuron* **79**, 461–477.
- 538 **Hand, R., Bortone, D., Mattar, P., Nguyen, L., Heng, J. I.-T., Guerrier, S., Boutt, E., Peters, E.,**
539 **Barnes, A. P., Parras, C., et al.** (2005). Phosphorylation of Neurogenin2 specifies the migration
540 properties and the dendritic morphology of pyramidal neurons in the neocortex. *Neuron* **48**, 45–62.
- 541 **Hasenpusch-Theil, K., Magnani, D., Amaniti, E.-M., Han, L., Armstrong, D. and Theil, T.** (2012).
542 Transcriptional analysis of Gli3 mutants identifies Wnt target genes in the developing hippocampus.
543 *Cereb Cortex* **22**, 2878–2893.
- 544 **Iulianella, A., Vanden Heuvel, G. and Trainor, P.** (2003). Dynamic expression of murine Cux2 in
545 craniofacial, limb, urogenital and neuronal primordia. *Gene Expr Patterns* **3**, 571–577.
- 546 **Lewandoski, M. and Martin, G. R.** (1997). Cre-mediated chromosome loss in mice. *Nat Genet* **17**,
547 223–225.
- 548 **Madisen, L., Zwingman, T. A., Sunkin, S. M., Oh, S. W., Zariwala, H. A., Gu, H., Ng, L. L.,**
549 **Palmiter, R. D., Hawrylycz, M. J., Jones, A. R., et al.** (2010). A robust and high-throughput Cre
550 reporting and characterization system for the whole mouse brain. *Nat Neurosci* **13**, 133–140.
- 551 **Mangale, V. S., Hirokawa, K. E., Satyaki, P. R. V., Gokulchandran, N., Chikbire, S.,**
552 **Subramanian, L., Shetty, A. S., Martynoga, B., Paul, J., Mai, M. V., et al.** (2008). Lhx2 selector
553 activity specifies cortical identity and suppresses hippocampal organizer fate. *Science* **319**, 304–309.
- 554 **Pattabiraman, K., Golonzhka, O., Lindtner, S., Nord, A. S., Taher, L., Hoch, R., Silberberg, S. N.,**
555 **Zhang, D., Chen, B., Zeng, H., et al.** (2014). Transcriptional regulation of enhancers active in
556 protodomains of the developing cerebral cortex. *Neuron* **82**, 989–1003.
- 557 **Srinivasan, S., Hu, J. S., Currle, D. S., Fung, E. S., Hayes, W. B., Lander, A. D. and Monuki, E. S.**
558 (2014). A BMP-FGF morphogen toggle switch drives the ultrasensitive expression of multiple genes
559 in the developing forebrain. *PLoS Comput. Biol.* **10**, e1003463.
- 560 **Tole, S., Ragsdale, C. W. and Grove, E. A.** (2000). Dorsoventral Patterning of the Telencephalon Is
561 Disrupted in the Mouse Mutant extra-toesJ. *Dev Biol* **217**, 254–265.
- 562 **Visel, A., Prabhakar, S., Akiyama, J. A., Shoukry, M., Lewis, K. D., Holt, A., Plajzer-Frick, I.,**
563 **Afzal, V., Rubin, E. M. and Pennacchio, L. A.** (2008). Ultraconservation identifies a small subset
564 of extremely constrained developmental enhancers. *Nat Genet* **40**, 158–160.
- 565 **Watanabe, M., Fung, E. S., Chan, F. B., Wong, J. S., Coutts, M. and Monuki, E. S.** (2016). BMP4
566 acts as a dorsal telencephalic morphogen in a mouse embryonic stem cell culture system. *Biology*
567 *Open* **5**, 1834–1843.
- 568 **Wilken, M. S., Brzezinski, J. A., La Torre, A., Siebenthal, K., Thurman, R., Sabo, P., Sandstrom,**
569 **R. S., Vierstra, J., Canfield, T. K., Hansen, R. S., et al.** (2015). DNase I hypersensitivity analysis
570 of the mouse brain and retina identifies region-specific regulatory elements. *Epigenetics Chromatin*
571 **8**, 8.
- 572 **Winkler, C. C., Yabut, O. R., Fregoso, S. P., Gomez, H. G., Dwyer, B. E., Pleasure, S. J. and**

- 573 **Franco, S. J.** (2018). The Dorsal Wave of Neocortical Oligodendrogenesis Begins Embryonically
574 and Requires Multiple Sources of Sonic Hedgehog. *J Neurosci* **38**, 5237–5250.
- 575 **Wittmann, W., Iulianella, A. and Gunhaga, L.** (2014). Cux2 acts as a critical regulator for
576 neurogenesis in the olfactory epithelium of vertebrates. *Dev Biol* **388**, 35–47.
- 577 **Zimmer, C., Tiveron, M.-C., Bodmer, R. and Cremer, H.** (2004). Dynamics of Cux2 expression
578 suggests that an early pool of SVZ precursors is fated to become upper cortical layer neurons.
579 *Cereb. Cortex* **14**, 1408–1420.
- 580

Figure 1 (Fregoso et al)

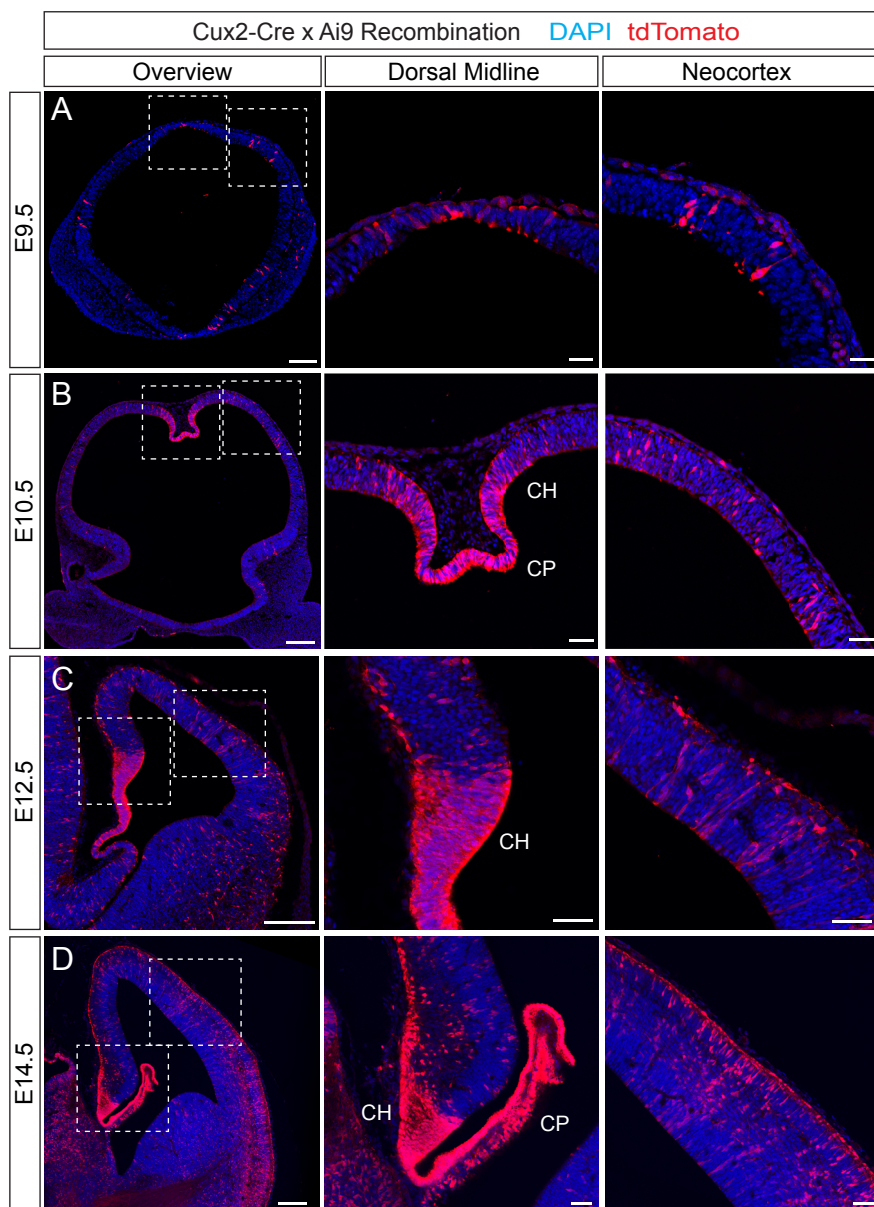
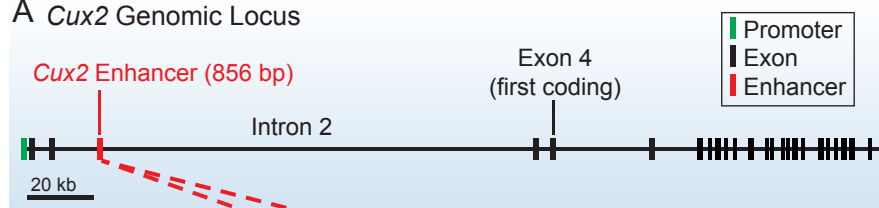


Figure 2 (Fregoso et al)

A *Cux2* Genomic Locus



B

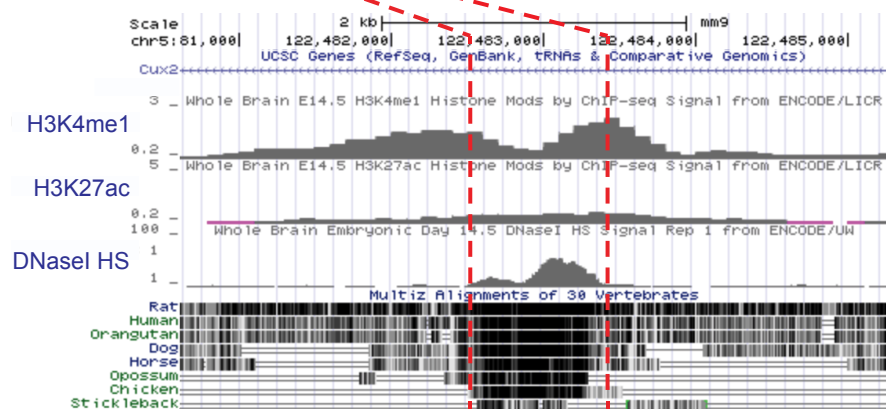


Figure 3 (Fregoso et al)

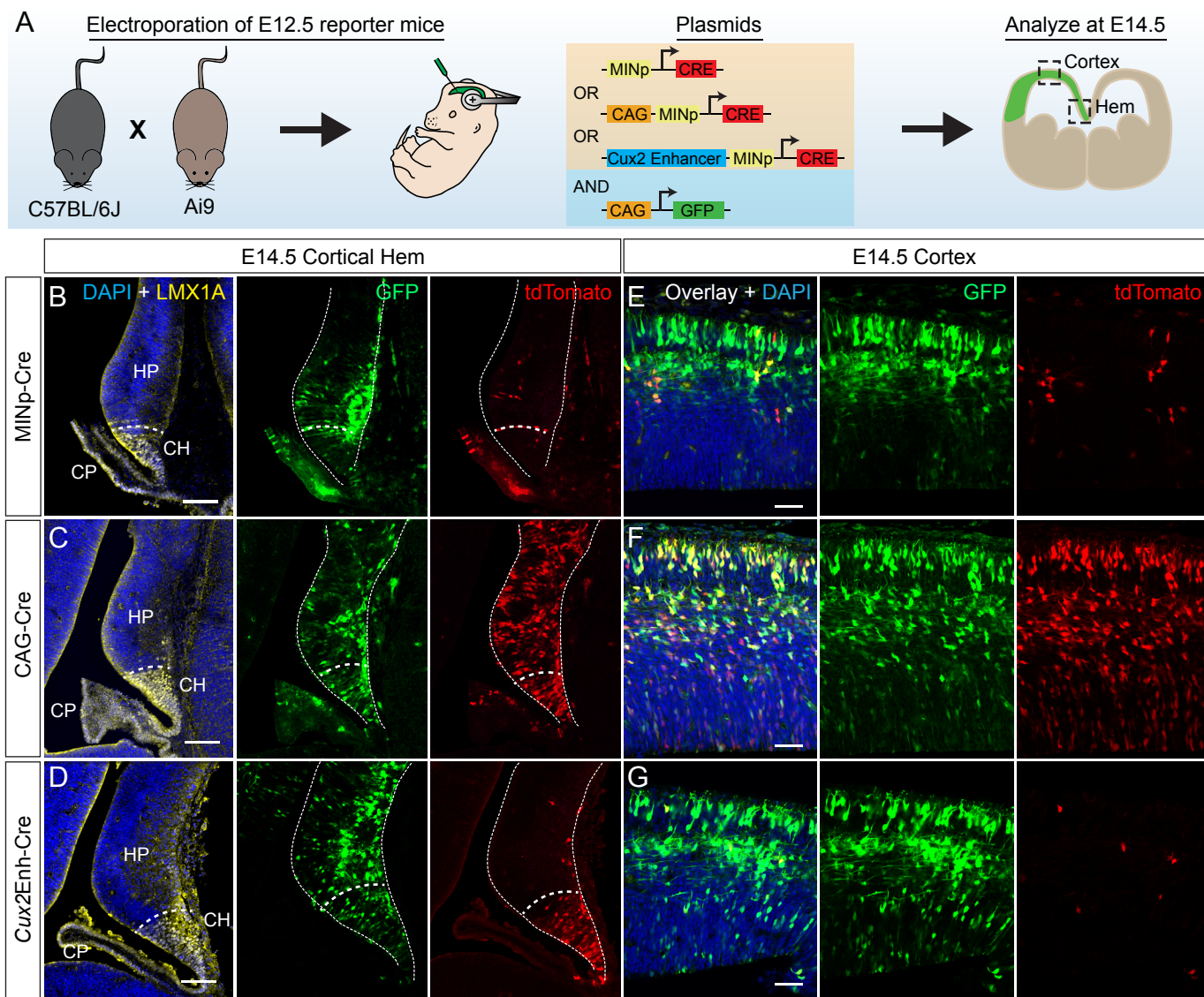


Figure 4 (Fregoso et al)

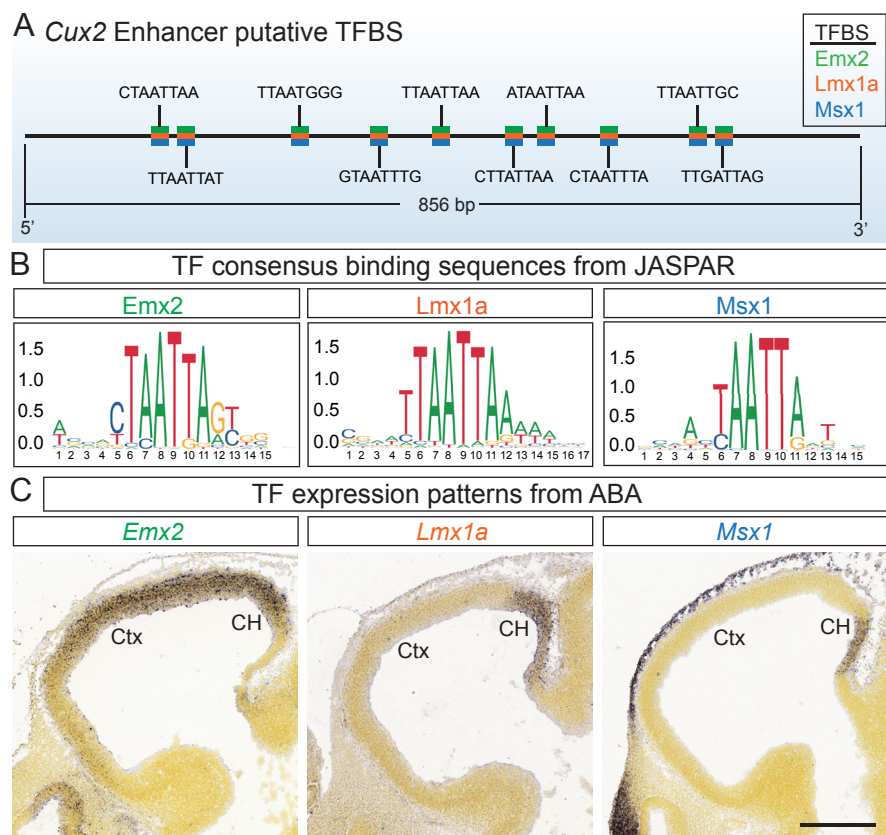


Figure 5 (Fregoso et al)

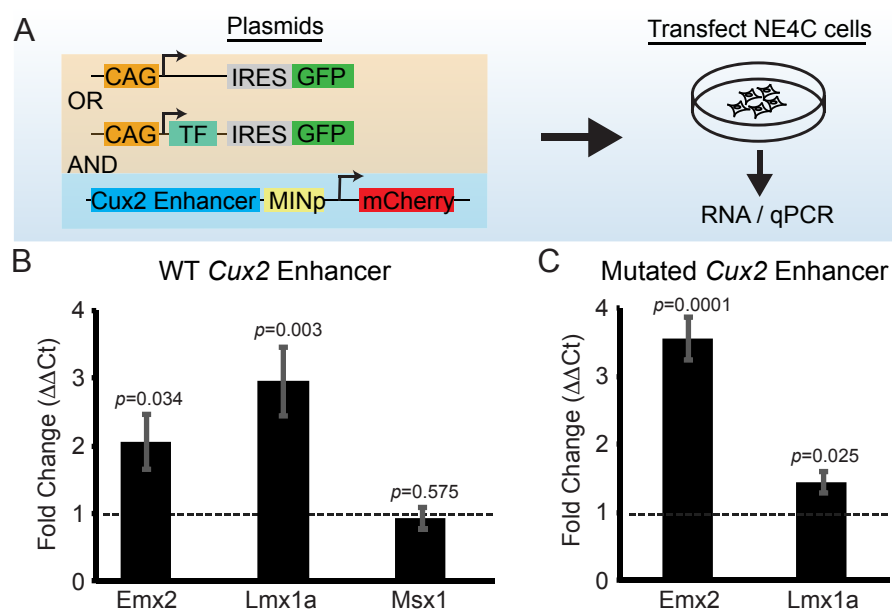


Figure 6 (Fregoso et al)

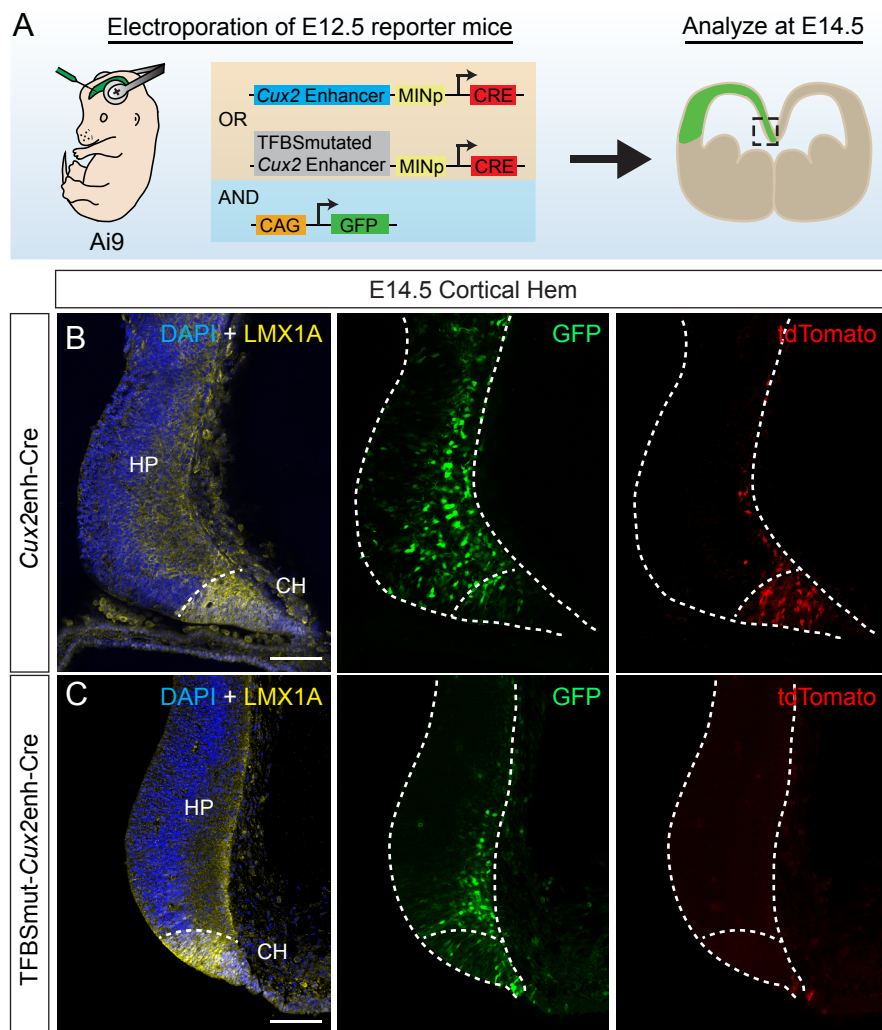


Figure 7 (Fregoso et al)

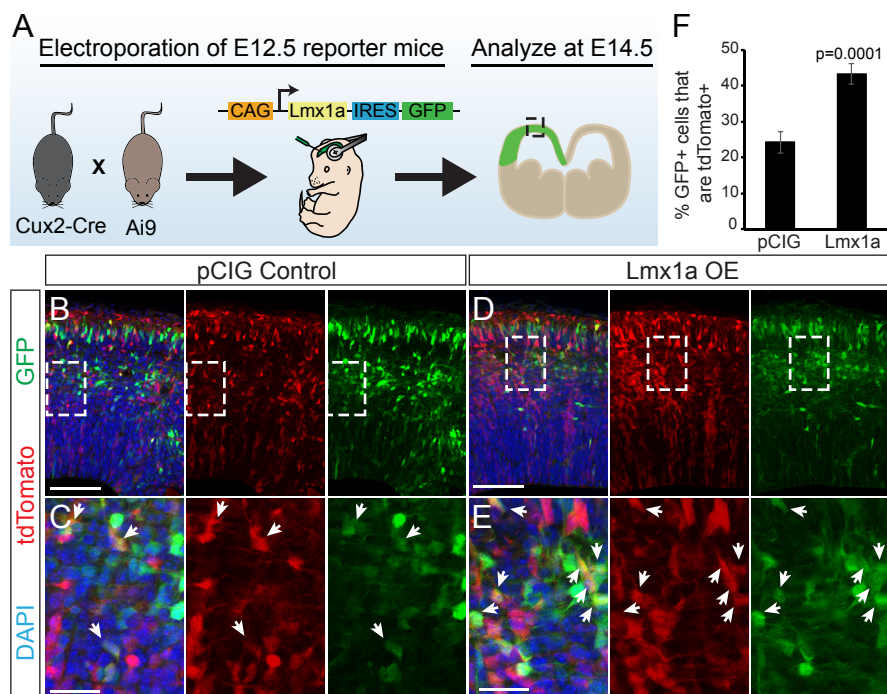


Figure 8 (Fregoso et al)

